*Continental Shelf Research*, Vol. 12, No. 7/8, pp. 891–906, 1992.
Printed in Great Britain.

0278–4343/92 $5.00 + 0.00




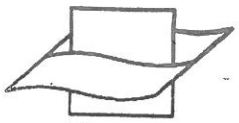



# A three-dimensional model of the water circulation around an island in shallow water

ERIC DELEERSNIJDER,* ALAIN NORRO† and ERIC WOLANSKI‡

(*Received* 24 *September* 1991; *accepted* 5 *February* 1992)

**Abstract**—A three-dimensional model is applied to the study of the tidal flow in the shallow waters around Rattray Island, Great Barrier Reef, Australia. The model uses the $\sigma$-coordinate system and the numerical procedure is based on the finite volume approach. Two counter-rotating eddies develop in the wake of the island. The shearing and veering of the horizontal velocity is predicted to be small, hence the vertical motions are negligible almost everywhere, with the exception of some small regions. In the center of the eddies important upwelling is found, which is in qualitative agreement with theory and observations. The model exhibits strong downwelling along the upstream side of the island. Overall, the magnitude of the computed vertical motions may be too small and it is hypothesized that this may be due to a lack of resolution of the model. Further improvements to the model are outlined.

## 1. INTRODUCTION

OVER recent years considerable attention has been devoted to the study of the water circulation in shallow coastal waters around coral reefs, islands and headlands. The studies have concentrated on the tidal eddies which form in the lee of these obstacles, trapping water and particulates. "This has important implications in the determination of the location of fisheries and in the siting of waste outfalls" (WOLANSKI *et al.*, 1984). These flows have zones of strong localized upwelling and downwelling which have important biological consequences linked to patchiness and aggregation processes around coral reefs. These recirculation zones thus have a significant impact on the marine environment. Hence, understanding their dynamics is an important issue.

Tidal eddies downstream of islands and headlands have been observed by many authors, such as PINGREE (1978), WOLANSKI *et al.* (1984), PATTIARATCHI *et al.* (1987), GEYER and SIGNELL (1990).

SIGNELL and GEYER (1991) explained that eddies form in the lee of sharp topographic features because of the flow separation occurring "where streamlines break away from the coast, carrying high vorticity fluid from the lateral boundary into the interior of the flow". The importance of unsteadiness has been emphasized by BLACK and GAY (1987). PINGREE

*G. Lemaître Institute of Astronomy and Geophysics (ASTR), Catholic University of Louvain, Chemin du Cyclotron 2, B-1348 Louvain-la-Neuve, Belgium.
†Oceanology Laboratory, Sart Tilman B6, University of Liège, B-4000 Liège, Belgium.
‡Australian Institute of Marine Science (AIMS), Cape Ferguson, PMB No. 3, Townsville M.O., Queensland 4810, Australia.

(1978) showed that, within the eddies, there is a balance between pressure gradient, centrifugal forces due to the curvature of the flow and Coriolis force. In addition, frictional effects induce a convergence of the flow near the bottom, resulting in upwelling at the center of the eddies (WOLANSKI *et al.*, 1984). Flow separation does not always lead to the formation of stable attached eddies. WOLANSKI *et al.* (1984) proposed to characterize the flow behind an island or a headland by the island wake parameter, $P$, which is a measure of the non-linear acceleration terms relative to the bottom friction. INGRAM and CHU (1987), PATTIARATCHI *et al.* (1987) and TOMCZAK (1988) confirmed the relevance of $P$. When $P \approx 1$, two attached eddies of size comparable to the island length are found (WOLANSKI, 1991). As $P$ increases, instabilities occur and the eddies give rise to meanders. For higher values of $P$, the meanders become unstable and small vortices are shed.

Depth-integrated models have been used to investigate the dynamics of the eddies described above (PINGREE and MADDOCK, 1980; FALCONER *et al.*, 1986; BLACK and GAY, 1987; WOLANSKI, 1988; SIGNELL, 1989; SIGNELL and GEYER, 1991). Those models proved to be very successful. In particular, FALCONER *et al.* (1986) made a thorough comparison of model results with the data collected by WOLANSKI *et al.* (1984) in the vicinity of Rattray Island, Great Barrier Reef, Australia (Fig. 1).

In general, shallow water eddies can thus be explained by two-dimensional dynamics. It does however not imply that there is no three-dimensional circulation in the eddies as suggested by observations (WOLANSKI *et al.*, 1984; WOLANSKI and HAMNER, 1988).

Recently, a three-dimensional model has been applied to the numerical simulation of the tidal flow around Rattray Island (DELEERSNIJDER *et al.*, 1989; DELEERSNIJDER and WOLANSKI, 1990) where $P \approx 1$. From the results of this model, the up- and down-welling zones are identified and the corresponding vertical motions are examined in the light of existing theory and observations.

## 2. DESCRIPTION OF THE MODEL

A version of GHER (University of Liège) three-dimensional marine hydrodynamics model was used (NIHOUL, 1984; NIHOUL and DJENIDI, 1987; DELEERSNIJDER and NIHOUL, 1988; NIHOUL *et al.*, 1989; BECKERS, 1991).

According to WOLANSKI *et al.* (1984) density effects are negligible near Rattray Island so that the water is considered to have constant density. On the vertical the hydrostatic balance is assumed. Moreover, the $\sigma$-coordinate is used in order to take into account bottom and surface topography. The physical time-space coordinates $(t, x_1, x_2, x_3)$ transform to new coordinates as follows

$$(\tilde{t}, \tilde{x}_1, \tilde{x}_2, \tilde{x}_3) = \left(t, x_1, x_2, x_3 = L\frac{x_3 + h}{\eta + h} = L\sigma\right) \tag{1}$$

where $t$ denotes time; $x_1$ and $x_2$ are horizontal coordinates; $x_3$ stands for the vertical coordinate, positive upwards; $h$ and $\eta$ represent the unperturbed sea depth and the sea surface elevation, respectively. In the transformed space, or $\sigma$-space, the sea depth, $L$, is constant. Along with (1), it is customary to introduce a new vertical velocity defined as

$$\tilde{u}_3 = D_t\tilde{x}_3 = LD_t\sigma \tag{2}$$

where $D_t$ denotes the material derivative operator

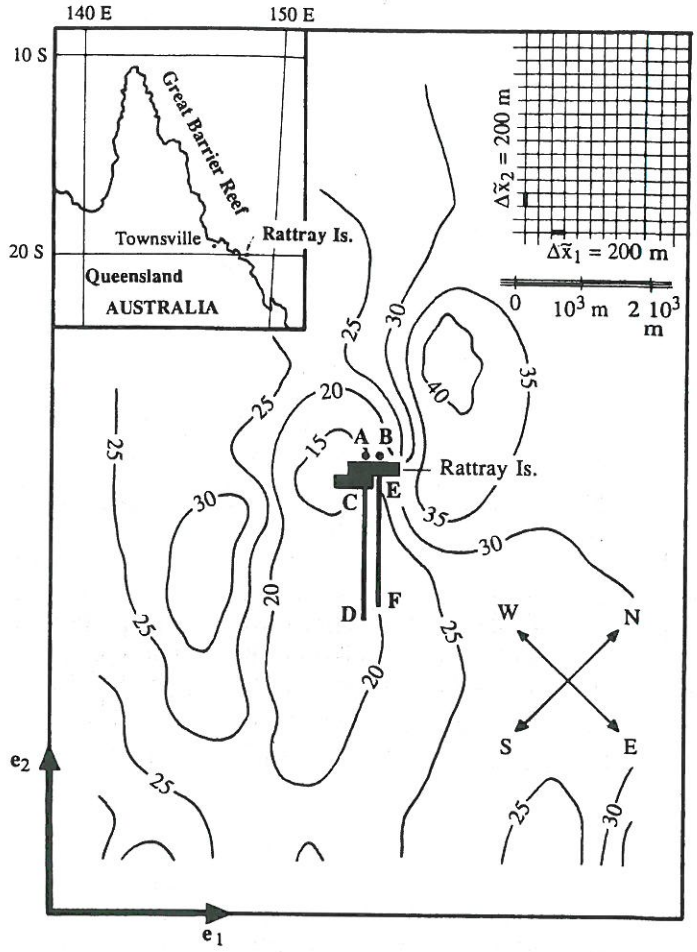


Fig. 1. Map of the computational domain. The location of Rattray Island in the Great Barrier Reef is illustrated in upper left corner. The computational grid is sketched in upper right corner. The sea depth, in meters, is indicated by means of iso-lines. Points A and B are referred to in Table 1. The planes of vertical section of Fig. 3 correspond to segments C–D and E–F.

$$D_t = \frac{\partial}{\partial t} + \mathbf{u}\cdot\nabla + u_3 \frac{\partial}{\partial x_3} \tag{3}$$

with $\nabla = \mathbf{e}_1\, \partial/\partial x_1 + \mathbf{e}_2\, \partial/\partial x_2$. Unit vectors $\mathbf{e}_1$ and $\mathbf{e}_2$ are horizontal. The horizontal and vertical velocity is denoted $\mathbf{u}$ and $u_3$, respectively. Introducing $\mathbf{e}_3 = \mathbf{e}_1 \times \mathbf{e}_2$, the total velocity reads

$$\mathbf{v} = \mathbf{u} + u_3\mathbf{e}_3. \tag{4}$$

One also defines the total depth of the sea in the physical space

$$H = h + \eta \tag{5}$$

the depth-averaged horizontal velocity

$$\langle \mathbf{u} \rangle = \frac{1}{H}\int_{-h}^{\eta} \mathbf{u}\, dx_3 = \frac{1}{L}\int_0^L \mathbf{u}\, d\tilde{x}_3 \tag{6}$$

and the deviation of the horizontal velocity relative to its depth-mean value

$$\mathbf{u}' = \mathbf{u} - \langle \mathbf{u} \rangle. \tag{7}$$

With the above assumptions and definitions, the governing equations of the model, in conservative form, read (DELEERSNIJDER *et al.*, 1989)

$$\frac{\partial \eta}{\partial \tilde{t}} + \tilde{\nabla} \cdot (H\langle \mathbf{u} \rangle) = 0 \tag{8}$$

$$\tilde{u}_3 = -\frac{1}{H}\int_0^{\tilde{x}_3} \tilde{\nabla} \cdot (H\mathbf{u}')\, d\tilde{x}_3 \tag{9}$$

$$\frac{\partial (H\mathbf{u})}{\partial \tilde{t}} + \tilde{\nabla} \cdot (H\mathbf{u}\mathbf{u}) + \frac{\partial (H\tilde{u}_3\mathbf{u})}{\partial \tilde{x}_3} + f\mathbf{e}_3 \times H\mathbf{u} = -gH\tilde{\nabla}\eta + \frac{\partial}{\partial \tilde{x}_3}\left(\frac{L^2}{H^2}\nu_T \frac{\partial (H\mathbf{u})}{\partial \tilde{x}_3}\right) + \mathbf{F}^{\mathbf{u}} \tag{10}$$

where $\tilde{\nabla} = \mathbf{e}_1\, \partial/\partial \tilde{x}_1 + \mathbf{e}_2\, \partial/\partial \tilde{x}_2$; $f$ is the Coriolis parameter ($f \approx -4 \times 10^{-5}\ \mathrm{s}^{-1}$); $g$ is the gravitational acceleration ($g \approx 9.8\ \mathrm{m\ s}^{-2}$); $\nu_T$ is the vertical eddy diffusivity; and $\mathbf{F}^{\mathbf{u}}$ is the horizontal diffusion term. The turbulence closure of GHER's model is of $k - \varepsilon$ type (NIHOUL and DJENIDI, 1987; NIHOUL *et al.*, 1989). However, in the exploratory phase, $\nu_T$ is computed by a more simple formulation that is possible because the flow under study is in shallow waters with negligible stratification (FISCHER *et al.*, 1979; DELEERSNIJDER *et al.*, 1989)

$$\nu_T = \kappa H\sigma(1 - \delta\sigma)u_* \tag{11}$$

where $\kappa$ is the von Karman constant ($\kappa \approx 0.4$); $\delta$ is an adjustable parameter, introduced by NIHOUL (1984) in the expression the mixing length, that is taken to be $\approx 0.6$; and $u_*$ is the bottom friction velocity, the square root of the norm of the bottom stress. It is worth noticing that, close to the sea bottom, (11) admits the following asymptotic expansion

$$\nu_T \sim \kappa H\sigma u_* \tag{12}$$

which allows for the existence of the logarithmic bottom boundary layer.

As stated by BLUMBERG and MELLOR (1987), horizontal diffusion of momentum is "usually required to damp small-scale computational noise". MELLOR and BLUMBERG (1985) showed that $\mathbf{F}^{\mathbf{u}}$ should only involve derivatives that are horizontal in the $\sigma$-space, i.e. $\partial/\partial \tilde{x}_1$ and $\partial/\partial \tilde{x}_2$. Elaborating on that theory, DELEERSNIJDER and WOLANSKI (1990) proposed a simple parameterization of $\mathbf{F}^{\mathbf{u}}$

$$\mathbf{F}^{\mathbf{u}} = \tilde{\nabla} \cdot [\tilde{\kappa}\tilde{\nabla}(H\mathbf{u}) + \tilde{\kappa}'\tilde{\nabla} \cdot (H\mathbf{u})\mathbf{I}] \tag{13}$$

with $\mathbf{I} = \mathbf{e}_1\mathbf{e}_1 + \mathbf{e}_2\mathbf{e}_2$ (identity tensor). The sensitivity of the model to diffusivities $\tilde{\kappa}$ and $\tilde{\kappa}'$ has been studied. It was shown that the extent of the eddies behind the island, as well as the intensity of the circulation within them, depends mainly on $\tilde{\kappa}$. On the other hand, $\tilde{\kappa}'$ was seen to be a parameter acting mainly on the noise in the vertical velocity field. Calibration against the data of WOLANSKI *et al.* (1984) led to $(\tilde{\kappa}, \tilde{\kappa}') = (2.5, 10)\ \mathrm{m^2\ s^{-1}}$.

## 3. BOUNDARY CONDITIONS AND MODEL'S IMPLEMENTATION

The flow around Rattray Island is mainly due to $M_2$ tide. Accordingly, at sea surface the wind stress is neglected

$$\left[\frac{L}{H}\nu_T\frac{\partial \mathbf{u}}{\partial \tilde{x}_3}\right]_{\sigma=1} = 0. \tag{14}$$

At sea bottom a slip condition is imposed. The bottom stress, $\tau^b$, is computed by the classical logarithmic "law of the wall"

$$\tau^b = \left[\frac{L}{H}\nu_T\frac{\partial \mathbf{u}}{\partial \tilde{x}_3}\right]_{\sigma=0} = \left[\frac{\kappa}{\ln(Z/z_0)}\right]^2 |\mathbf{u}(Z)|\,\mathbf{u}(Z) \tag{15}$$

where $Z$ is the height above sea bottom of the first grid point where $\mathbf{u}$ is defined; $z_0$ is the bottom roughness length, which, for the domain of interest, is equal to $5 \times 10^{-3}$ m (BLACK and GAY, 1987).

The impermeability of the sea surface and the sea bottom requires

$$[\tilde{u}_3]_{\sigma=0,1} = 0. \tag{16}$$

The tidal ellipses of the free steam, i.e. the flow outside the influence of Rattray Island, are strongly polarized (WOLANSKI *et al.*, 1984). Consequently, one horizontal axis, namely the $\tilde{x}_2$-axis, is prescribed to be parallel to the major axis of the tidal ellipses (Fig. 1). Furthermore, the transport across the lateral boundaries parallel to the free stream—the left-hand and right-hand side boundaries in Fig. 1—is fixed to zero

$$[\langle \mathbf{u} \rangle \cdot \mathbf{e}_1]_{\text{boundary}} = 0. \tag{17}$$

At the "lower boudary"—in Fig. 1—the normal depth-averaged velocity is prescribed according to *in situ* measurements, with

$$-0.5\ \text{m s}^{-1} \lesssim [\langle \mathbf{u} \rangle \cdot \mathbf{e}_2]_{\text{boundary}} \lesssim 0.5\ \text{m s}^{-1}. \tag{18}$$

At the "upper boundary" the observed sea surface elevation is imposed, with

$$[\eta_{\max} - \eta_{\min}]_{\text{boundary}} \approx 2\ \text{m}. \tag{19}$$

It must be stressed that the above boundary conditions only pertain to depth-independent quantities. Along the boundaries, $\mathbf{u}'$ is computed by a simplified form of the momentum equations, in which the derivatives of the velocity normal to the relevant boundary are cancelled. With such a practice, the model is allowed to compute its own shearing and veering at the boundaries, avoiding spurious up- or down-wellings which may arise when the imposed deviation of the horizontal velocity is not in agreement with that provided by the model in the interior of the computational domain (DELEERSNIJDER *et al.*, 1989).

The equations (8)–(10) were discretized on a three-dimensional staggered C grid according to the finite volume approach (PEYRET and TAYLOR, 1983). The time stepping of the surface gravity wave terms was the forward–backward scheme (MESINGER and ARAKAWA, 1976). The vertical turbulent fluxes of momentum were computed implicitly to prevent numerical instability.

Initially, the bathymetry of the model was that of FALCONER *et al.* (1986). This bottom

topography exhibits abrupt jumps of depth to which a two-dimensional model seems to be rather insensitive. In the three-dimensional model, however, the sharp depth changes induced much numerical noise in $\mathbf{u}'$ and thus in $\tilde{u}_3$. A numerical filter was applied to the original bathymetry to produce that displayed in Fig. 1. Interestingly, it turned out that it was more efficient to smooth $\ln h$ instead of $h$ itself.

The numerical grid comprised 41 × 59 "active" grid boxes on the horizontal and five levels in the vertical direction. The horizontal space increments were $\Delta\tilde{x}_1 = \Delta\tilde{x}_2 = 200$ m and the time step, constrained by the CFL condition on gravity waves, was $\Delta\tilde{t} = 5$ s.

## 4. MODEL RESULTS

In order to investigate the effect of different parameters and terms of the governing equations a series of numerical experiments on the tidal flow around Rattray Island was performed. They are reported in DELEERSNIJDER *et al.* (1989) and DELEERSNIJDER and WOLANSKI (1990). Here one discusses the results of the simulation that is expected to be in closest agreement with the reality.

### 4.1. *Horizontal velocity field*

During the falling tide, two counter-rotating eddies form in the wake of the island—in the upper part of Fig. 1. So far no current meters have been deployed in this region but aerial photography suggests the existence of these eddies (WOLANSKI *et al.*, 1984).

Similarly, during the rising tide, eddies develop behind the southeastern side of Rattray Island. Figure 2a shows the depth-integrated horizontal velocity field 11 h after high tide. The asymmetry of the eddies is due to bathymetry effect. Indeed, if one runs the model with flat bathymetry two eddies of similar shape form in the wake of the island.

Coriolis force is included in the model but is not important because the tidal period (≈0.5 day) is much shorter than the inertial period ($2\pi/f \approx 1.8$ days) and because the Rossby number, based on the island length, is large (TOMCZAK, 1988). Hence, any asymmetry in the development of tidal eddies in the domain may not be ascribed to the Coriolis force, as is the case in PINGREE's (1978) study.

Overall, $\langle \mathbf{u} \rangle$ is very close to that obtained by the two-dimensional model of FALCONER *et al.* (1986). Since the latter has been thoroughly validated it is assumed that the depth-averaged velocity field provided by the three-dimensional model described here is satisfactory.

The deviation of the horizontal velocity, $\mathbf{u}'$, relative to its depth-mean value, $\langle \mathbf{u} \rangle$, is very small as examplified in Fig. 2b. This may be quantified as follows. The root mean square of $|\mathbf{u}|$ taken over the whole computational domain is

$$|\mathbf{u}|_{\mathrm{RMS}} = 3.3 \times 10^{-1}\ \mathrm{m\,s^{-1}} \tag{20}$$

while

$$|\mathbf{u}'|_{\mathrm{RMS}} = 3.2 \times 10^{-2}\ \mathrm{m\,s^{-1}}. \tag{21}$$

Thus, at most locations $|\mathbf{u}'| \approx |\langle \mathbf{u} \rangle|/10$, justifying that two- and three-dimensional models give similar results for the depth-integrated velocity. There is some experimental evidence that the shearing and veering of the horizontal velocity are small (Fig. 3).

4.2. *Vertical velocity field*

From equations (1), (2), (8) and (10), it can be seen that $\eta$ and $\mathbf{u}$ do not depend upon $L$ (the water depth in the $\sigma$-space). However, the vertical velocity $\tilde{u}_3$ is proportional to $L$. Hence, if one prescribes that $L$ is equal to the horizontal characteristic length scale, $10^3$ m say, the computational domain in the $\sigma$-space will be isotropic. There is thus the potential that $\tilde{u}_3$ and $\mathbf{u}$ may have the same magnitude. Nevertheless, the model leads to

$$|\tilde{u}_3|_{\mathrm{RMS}} = 3.2 \times 10^{-3}\ \mathrm{m\ s^{-1}} \tag{22}$$

and

$$\frac{|\tilde{u}_3|_{\mathrm{RMS}}}{|\mathbf{u}|_{\mathrm{RMS}}} \approx 10^{-2}. \tag{23}$$

This result follows logically from a scaling of equations (9), (20) and (21). As a consequence, the vertical advection of momentum plays in general no role in the circulation around Rattray Island. It is however possible that, at particular locations, the

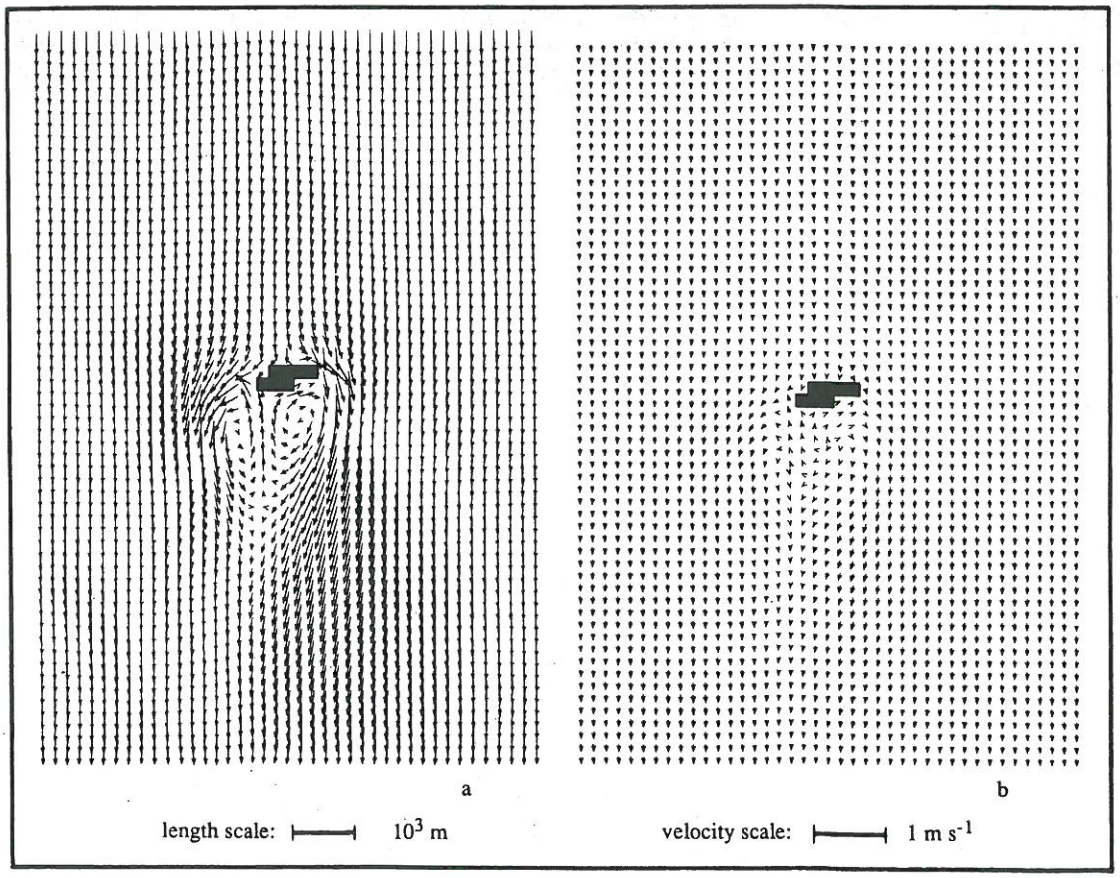


Fig. 2. (a) Depth-averaged horizontal velocity, $\langle \mathbf{u} \rangle$, 11 h after high tide. (b) Deviation of the horizontal velocity relative to $\langle \mathbf{u} \rangle$, illustrated by the difference between $\mathbf{u}'$ in the surface grid box and $\mathbf{u}'$ in the bottom one.

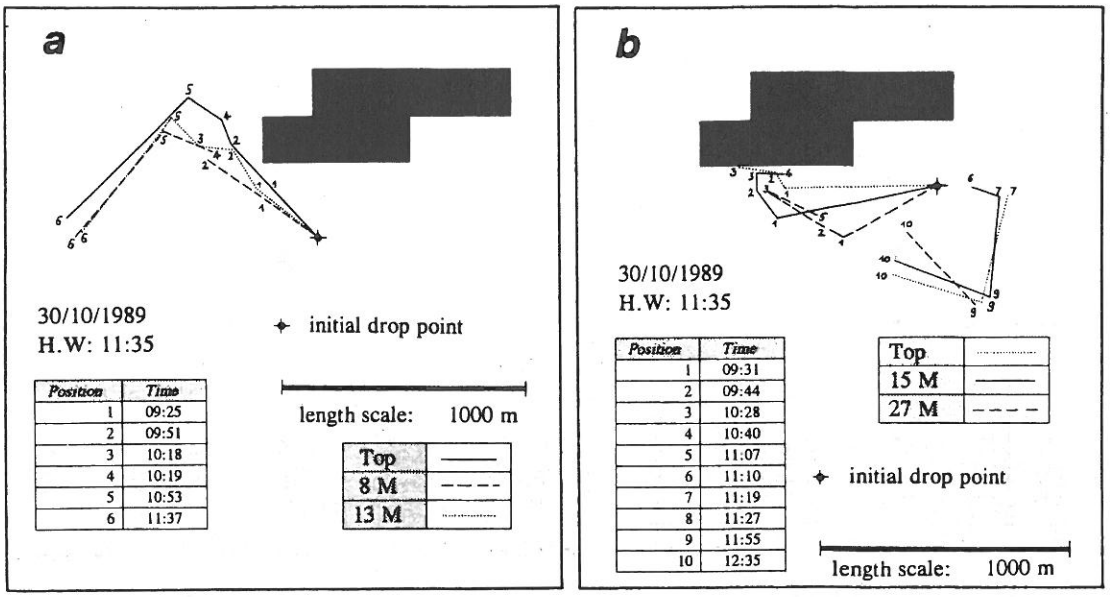


Fig. 3. Trajectories of drogues released in the lee of Rattray Island at various positions in the water column: 0, 8 and 13 m (a) and 0, 15 and 27 m (b) below the sea surface. The initial time ($t = 0$) is at high tide. In (b), the drogues, after hitting the sea bottom or the island, were redeployed. These data clearly suggest that the deviation of the horizontal velocity relative to its depth-mean is small.

ratio $|\tilde{u}_3|/|\mathbf{u}|$ may be much larger than $10^{-2}$ and that the vertical velocity may be locally quite important.

One must bear in mind that $\tilde{u}_3$ is very different from $u_3$, the real vertical velocity. In fact, one may write (DELEERSNIJDER, 1989)

$$u_3 = w_{UW} + w_{US} \tag{24}$$

with

$$w_{UW} = \frac{H}{L}\tilde{u}_3 \tag{25}$$

and

$$w_{US} = \sigma\frac{\partial \eta}{\partial t} - \mathbf{u}\cdot[(1-\sigma)\nabla h - \sigma\nabla\eta]. \tag{26}$$

It may be shown that a particle whose velocity is $\mathbf{u} + w_{US}\mathbf{e}_3$ does remain at the same relative height in the water column, i.e. this particle does not cross any iso-$\sigma$ surface. The sea surface and the sea bottom being iso-$\sigma$ surfaces, one may thus view $w_{US}$ as the vertical velocity of a particle adapting its motion to the geometry of the basin. Therefore, it is suggested to call $w_{US}$ the upsloping velocity. On the other hand, $w_{UW}$ is the velocity at which a fluid parcel crosses iso-$\sigma$ surfaces. As a matter of fact, $w_{UW}$ is not directly induced by sea surface or sea bottom topography and thus quantifies the actual up- or down-welling, i.e. a motion by which a particle comes relatively closer to the surface or the bottom by crossing iso-$\sigma$ surfaces.

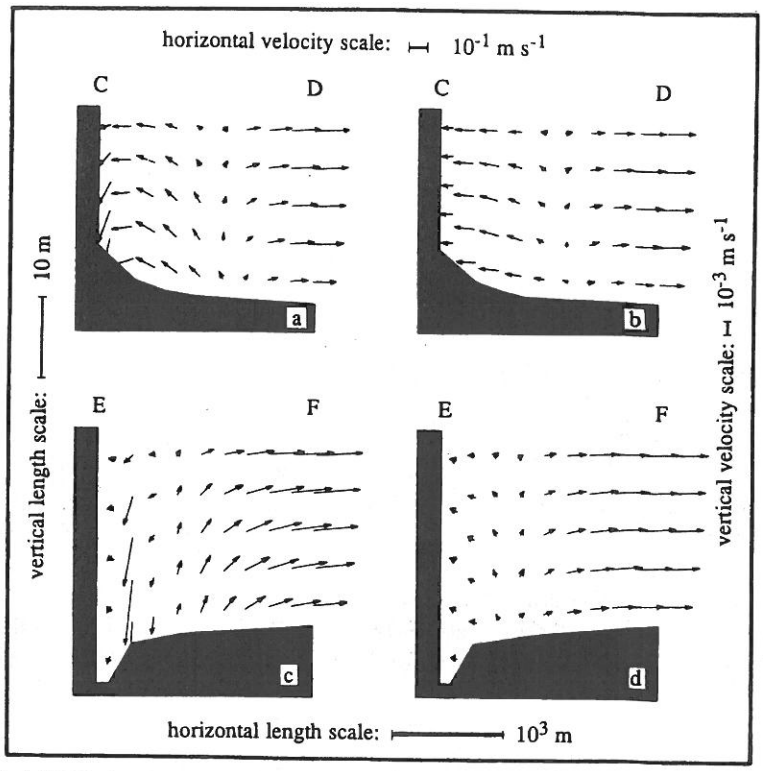


Fig. 4. (a) (c) Velocity $u_2\mathbf{e}_2 + w\mathbf{e}_3$ in the vertical sections C–D and E–F, respectively, as given in Fig. 1. (b) (d) Velocity $u_2\mathbf{e}_2 + w_{UW}\mathbf{e}_3$ in the vertical sections C–D and E–F, respectively. The difference between (a) and (c) or between (b) and (d) is due to the upsloping velocity, the vertical velocity induced by the bathymetry of the domain.

The upwelling velocity, $w_{UW}$, is not the vertical velocity one would obtain by running the model with a flat bathymetry. Thus, $w_{UW}$ actually depends upon the bottom topography, but not in a direct manner.

In the vertical sections of Fig. 4 it is shown that $|w_{US}| \gtrsim |w_{UW}|$, as is the case in the whole computational domain. The relative weakness of $w_{UW}$ is discussed below.

Here, one is chiefly interested in actual upwellings, and thus in $w_{UW}$ or, by virtue of (25), in $\tilde{u}_3$. Most of the vertical profiles of $\tilde{u}_3$ do not exhibit any change of sign. In other words, $|\tilde{u}_3|$ is zero at the bottom, increases to its maximum somewhere near the middle of the water column and decreases to zero at the surface, according to (16). One may thus characterize the actual upwelling motion by $\tilde{u}_3$ at mid-depth. Taking into account that the tidal eddies exist, with a significant intensity, for approximately 3 h, it seems appropriate to define

$$\Delta\sigma = \left[\frac{\tilde{u}_3}{L}\right]_{\sigma=0.5} \times 3\,\mathrm{h} \tag{27}$$

which is the fraction of the water column travelled—during the lifetime of an eddy—by a fluid parcel whose vertical velocity is $[w_{UW}]_{\sigma=0.5}$.

The horizontal distribution of $\Delta\sigma$ at 11 h after high tide, i.e. at the same instant as the

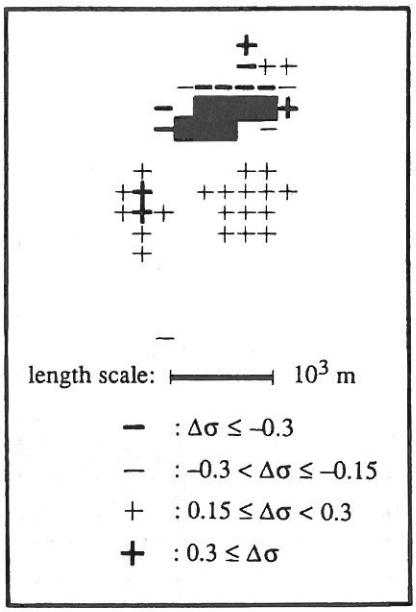


Fig. 5. Horizontal distribution around Rattray Island at flood tide of the upwelling parameter $\Delta\sigma$, defined in equation (27) and indicating the fraction of the water column travelled by a water parcel in 3 h.

velocity field given in Fig. 2, is shown in Fig. 5. Figures 4 and 5 indicate that there is an important upwelling in the eddies located downstream of Rattray Island, and that there is a downwelling in a narrow band on the upstream and, to a lesser degree, on the downstream side of the island. In the rest of the computational domain, the vertical motions are definitely negligible.

Overall, the horizontal extent of the up- and down-welling regions is rather small.

### 4.3. *Vertical motions in the eddies*

By analogy with the flow in a stirred tea cup, previous models of the internal circulation of tidal eddies in shallow waters (WOLANSKI *et al.*, 1984; TOMCZAK, 1988) have assumed the existence of an Ekman benthic boundary layer at the base of the wake recirculation region, from the theory of rotating fluid over a solid boundary (GREENSPAN, 1968). Accordingly, the secondary circulation in the eddies, if the water is entrapped in these eddies, comprises a convergence towards the center of the eddy near the bottom, an upwelling in the center, a divergence near the surface and downwelling near the edge. VON RIEGELS (1938) and VAN SENDEN (1987) studied such eddies in laboratory experiments and found indeed upwelling near the eddy center. Field evidence using plankton and coral eggs as a tracer points to the existence of an upwelling near the center and downwelling along the edges (HAMNER and HAURI, 1977; ALLDREDGE and HAMNER, 1980; HAMNER and WOLANSKI, 1988; WOLANSKI and HAMNER, 1988). Our model however shows negligible downwelling along the edges of the eddy except along the solid boundaries (the island walls), where some downwelling is predicted. This model result suggests that tidal eddies are not completely isolated from the free stream currents, and that no downwelling is actually required. This is an important difference with the tea cup flow, where downwelling takes

place along the walls so as to balance the upwelling at the center. One must point out that the vertical water flux integrated over the eddies' upwelling zone is rather small so that the corresponding horizontal convergence–divergence fluxes may remain unnoticed in current meters records in the presence of a very strong tidal current.

One might object that the unsteadiness is another major difference between the tidal flow and the classical tea cup problem. This is however not correct. On the one hand, the importance of advection relative to local acceleration is measured by the Keulegan and Carpenter number, $K_c$ (SIGNELL and GEYER, 1991). In the present case, $K_c \approx 5$, which means that unsteadiness is important, but not dominant. On the other hand, unsteadiness is related to mass conservation through the motion of the sea surface, which is only concerned with $\langle \mathbf{u} \rangle$, while $\tilde{u}_3$ mainly depends on $\mathbf{u}'$ (since $|\eta| \ll h$), as indicated by (9). Thus, the unsteadiness cannot account for the absence of downwelling near the edge of the eddies.

In the light of the present discussion it seems appropriate to revise the scenario of the secondary circulation within tidal eddies, abandoning the closed circulation assumption and turning to an open circulation model involving only upwelling at the center of the eddy and some downwelling along the upstream side of the island. The analogy with the flow in a tea cup holds only for the upwelling in the center of the eddy and the—rather small—downwelling along the downstream side of the island.

The dimensional analysis performed by WOLANSKI *et al.* (1984) is still valid, since it does not rely on a possible influence of the vertical velocity on the momentum balance. As a consequence, there is no reason to question the relevance of the island wake parameter.

WOLANSKI *et al.* (1984) found that the water trapped in the eddies behind Rattray Island is somewhat cooler than the water outside the eddies. This observation does not imply complete trapping and, hence, does not clash with our predictions that a weak cross-flow may exist. The observation of different temperature in the eddies may be explained by the advection of a horizontally varying temperature field, warmer water being transported past the island as the flood tide progresses. A transient trapping occurs when vortex lines shed behind the separation points of Rattray Island become unstable and fold unto themselves, temporarily trapping water in an eddy (SIGNELL, 1989). During that time, warmer water is carried past Rattray Island so that the water in the eddies eventually appears cooler.

An examination of the horizontal temperature distribution in the lee of Rattray Island (WOLANSKI *et al.*, 1984) suggests cold eddy water being advected downstream away from the eddy, supporting the hypothesis that the circulation in tidal eddies is not closed.

### 4.4. *Vertical motions upstream of the island*

Most of the studies carried out so far focused on the circulation downstream of the islands. As a result, almost nothing is known about upstream hydrography.

The present three-dimensional model predicts important downwelling in a narrow strip upstream of the island (Fig. 5). Whether or not this downwelling is in agreement with existing observations is unclear. The results of the model however permit a basic understanding of the mechanism of this downwelling.

Vertical velocity $\tilde{u}_3$ may be decomposed into two components

$$\tilde{u}_3 = \tilde{u}_{3,1} + \tilde{u}_{3,2} \tag{28}$$

*Table 1. Decomposition of $\tilde{u}_3$ into $\tilde{u}_{3,1}$ and $\tilde{u}_{3,2}$ at locations A and B, respectively, as given in Fig. 1. The vertical velocities are given in $10^{-2}$ m s$^{-1}$*

| | (a) | | | | (b) | | |
|---|---|---|---|---|---|---|---|
| $\sigma$ | $\tilde{u}_{3,1}$ | $\tilde{u}_{3,2}$ | $\tilde{u}_3$ | $\sigma$ | $\tilde{u}_{3,1}$ | $\tilde{u}_{3,2}$ | $\tilde{u}_3$ |
| 0.9 | −0.7 | −1.0 | −1.7 | 0.9 | 0.3 | −1.7 | −1.4 |
| 0.7 | −1.9 | −2.9 | −4.8 | 0.7 | 0.8 | −4.5 | −3.7 |
| 0.5 | −2.4 | −4.3 | −6.7 | 0.5 | 1.0 | −6.0 | −5.0 |
| 0.3 | −1.8 | −4.6 | −6.4 | 0.3 | 0.6 | −5.3 | −4.7 |
| 0.1 | −0.6 | −2.2 | −2.8 | 0.1 | 0.2 | −2.2 | −2.0 |

where

$$\tilde{u}_{3,i} = -\frac{1}{H}\int_0^{\tilde{x}_3} \frac{\partial}{\partial \tilde{x}_3}(Hu_i')\, d\tilde{x}_3, \quad (i = 1, 2) \tag{29}$$

with

$$[\tilde{u}_{3,i}]_{\sigma=0,1} = 0, \quad (i = 1, 2). \tag{30}$$

In the downwelling band upstream of Rattray Island $-\tilde{u}_{3,2} \gg |\tilde{u}_{3,1}|$, as exemplified in Table 1. Thus, the downwelling is mostly due to variations of $Hu_2'$ in the $\tilde{x}_2$ direction, which is the direction of the free stream. Because of the effect of the bottom friction (Beckers, personal communication), near the surface

$$-Hu_2' \geq 0, \quad \sigma \to 1 \tag{31}$$

and, close to the bottom,

$$-Hu_2' \leq 0, \quad \sigma \to 0. \tag{32}$$

Since $Hu_2'$ is zero at the coast, reasoning from (29)–(32), one may then conjecture that

$$\tilde{u}_{3,2} \leq 0, \quad 0 \leq \sigma \leq 1. \tag{33}$$

The above inequality may be seen to be rigorously valid if it is further assumed that $Hu_2'$ has only one change of sign over the whole water column, which is often true—one must bear in mind that $Hu_i'$ must have, at least, one change of sign since $\langle Hu_i \rangle = 0$. The downwelling is mostly due to $\tilde{u}_{3,2}$ because the derivatives in the direction of the free stream clearly dominate those in the perpendicular direction close to the upstream face of the island. This is no longer valid near the tips of the island, which may be the reason that the downwelling is weaker as the tips are approached (Fig. 5).

The downwelling strip is preceded by a region where the $\tilde{u}_3$ field is rather noisy (DELEERSNIJDER and WOLANSKI, 1990), but overall dominated by upwelling, of which the significance may be questioned. The upstream region is associated with very high variations of the velocity, which generally results in the generation of important numerical noise (JAMES, 1986). The occurrence of this noise can be prevented by the use of an appropriate numerical scheme (JAMES, 1986), of which a simple, but not fully satisfactory, version is already implemented (DELEERSNIJDER *et al.*, 1989).

4.5. *Magnitude of the vertical motions*

In the up- and down-welling zones identified in Fig. 5, one generally has

$$|\Delta\sigma| \lesssim 0.4. \tag{34}$$

For instance, the upward distance travelled by a particle trapped in an eddy will not exceed four tenths of the water height during the lifetime of the eddy. In most cases, this distance is even significantly smaller.

One may imagine that the model actually underestimates the magnitude of the upwelling velocity, because of the use of a too coarse grid. Utilizing a finer grid would allow the representation of sharper gradients, which would possibly result in higher vertical velocities. The basic question is thus whether the grid is too coarse or not. Looking at Fig. 2a, one sees that there are no more than three grid boxes on the width of the left eddy, and no more than five on the width of the other. Furthermore, DELEERSNIJDER and WOLANSKI (1990) computed the horizontal length scales of $\mathbf{u}$ and $\tilde{u}_3$ in a small domain encompassing Rattray Island according to a formula given by POWELL (1989). Scales not exceeding 600 m were found, which confirms the fact that a mesh size of 200 m may lead to underestimating the vertical velocities. This is a constraint due to limited computer power and the need to include in the model both the undisturbed far-field and the complex flow near the island.

Direct *in situ* measurements of the vertical velocity are presently impracticable. But, it is possible to measure vertical profiles of $\mathbf{u}'$. If those measurements confirm the relative smallness of $\mathbf{u}'$, then the overall smallness of $\tilde{u}_3$ will be, at least partly, validated. But, if the latter is true, it does not imply that $\tilde{u}_3$ is small everywhere. Indeed, $\mathbf{u}'$, even small, may exhibit very sharp gradients, which could result in significant upwelling velocity, as indicated by Equation (9). Thus, if $\mathbf{u}'$ is indeed small compared with $\langle\mathbf{u}\rangle$, any region where the vertical motions are important must be of small horizontal extent. This is clearly suggested by the results presented here, despite a definite lack of horizontal resolution.

For significant upwelling to take place in a given eddy within one tidal cycle, $|\Delta\sigma|$ must be of order 1. If this is actually the case in nature, i.e. if the real $\tilde{u}_3$ is 2 to 3 times higher than the present one, the ratio $|\tilde{u}_3|/|\mathbf{u}|$ will be of order 1 in the center of the eddies and in the downwelling strip upstream of Rattray Island. Even in this case, the vertical velocity will not have much effect on the overall flow, for the regions where the upwelling velocity will be significant are very small. This is confirmed by a numerical experiment in which the vertical advection term of the momentum equation was simply multiplied by three.

If the actual magnitude of $\Delta\sigma$ eventually turns out to be less than one, it would not mean that vertical motions are definitely unimportant. One must bear in mind that most of the particles of biological interest are buoyant, i.e. they are associated with a positive migration velocity because of Archimede's force. Thus, the vertical displacement of buoyant particles is due to the sum of the hydrodynamic vertical velocity and their own migration velocity. Coral eggs, for instance, are more buoyant than most eggs from animals that have a planktonic stage so that they tend to float, even in areas of downwelling. In these regions, because of the surface convergence associated with downwelling, the most buoyant particles will aggregate near the surface (WOLANSKI and HAMNER, 1988) while less buoyant particles may be distributed through the water column, depending on the magnitude of the downwelling velocity and their buoyancy.

There is biological evidence for surface accumulation of buoyant material (LAFOND and

LAFOND, 1971; HAMNER and HAURI, 1981) upstream of obstacles. This could support the model results that indicate downwelling upstream of Rattray Island.

## 5. CONCLUSION

Future developments of the three-dimensional model must obviously include the refinement of the horizontal grid.

Since the upwelling velocity mainly depends on $\mathbf{u}'$, the prediction of the vertical fluxes of momentum must be improved. To do so, the full $k$-$\varepsilon$ turbulence closure of GHER's model will be implemented so as to provide more accurate eddy diffusivity profiles. To allow the introduction of a sophisticated turbulence model, the vertical resolution must be, at least, doubled, to have no less than 10 grid boxes on each vertical.

In the future, the model should be used to predict, in three dimensions, the fate of particulates of biological interest around coral reefs and islands. This is particularly important since the particulates at stake usually have some positive buoyancy (which in some cases can be considerable, e.g. coral eggs) so that zones of upwelling near the eddy center are zones of strong horizontal dispersion (SIGNELL, 1989), and zones of downwelling are zones of aggregation (WOLANSKI and HAMNER, 1988). These aggregation zones are crucial since they imply that particulates do not disperse over a vast area, but are instead aggregated as if negative diffusion occurred. Present numerical models of the fate of particulates around coral reefs neglect these key processes. Thus, the computation of trajectories of lagrangian tracers of various buoyancy should be implemented as an important field for future research.

All the improvements listed above will require computer resources that are one order of magnitude larger than those needed to obtain the results presented here.

The results of the three-dimensional model are very encouraging. The depth-integrated velocity field is in agreement with the observations. The model predicts upwelling in the center of the tidal eddies, which is in qualitative agreement with both theory and observations. Important downwelling, possibly preceded by upwelling, is predicted upstream of the island. Overall, the magnitude of the vertical motions may be too small, but it is believed that this may be due to a lack of horizontal resolution.

*Acknowledgements*—Part of the work discussed here was done when Eric Deleersnijder and Alain Norro were, respectively, Research Assistant at the National Fund for Scientific Research of Belgium and Ph.D. fellow at the Australian Institute of Marine Science. Alain Norro gratefully thanks the Captain, the Officers and the crew of H.M.A.S. *Geralton* for their help with the experimental part of this study. The support and comments of Professor J. C. J. Nihoul are acknowledged. André Joris was of great help in the preparation of the figures.

## REFERENCES

ALLDREDGE A. L. and W. L. HAMNER (1980) Recurring aggregation of zooplankton by a tidal current. *Estuarine and Coastal Marine Science*, **10**, 31–37.

BECKERS J. M. (1991) Application of the GHER 3D general circulation model to the Western Mediterranean. *Journal of Marine Systems*, **1**, 315–332.

BLACK K. P. and S. L. GAY (1987) Eddy formation in unsteady flows. *Journal of Geophysical Research*, **92**, 9514–9522.

BLUMBERG A. F. and G. L. MELLOR (1987) A description of a three-dimensional coastal ocean circulation model. In: *Three-dimensional coastal ocean models*, N. S. HEAPS, editor, American Geophysical Union, Washington, D.C., pp. 1–16.

DELEERSNIJDER E. (1989) Upwelling and upsloping in three-dimensional marine models. *Applied Mathematical Modelling*, **13**, 462–467.

DELEERSNIJDER E. and J. C. J. NIHOUL (1988) *General circulation in the Northern Bering Sea*, ISHTAR Annual Progress Report, University of Liège, 392 pp.

DELEERSNIJDER E. and E. WOLANSKI (1990) Du rôle de la dispersion horizontale de quantité de mouvement dans les modèles marins tridimensionnels. In: *Journées numériques 1990—Courants océaniques*, J. M. CROLET and P. LESAINT, editors, Publications mathématiques de Besançon, pp. 39–50.

DELEERSNIJDER E., E. WOLANSKI and A. NORRO (1989) Numerical simulation of the three-dimensional tidal circulation in an Island's wake. In: *Computers and experiments in fluid flow*, G. M. CARLOMAGNO and C. A. BREBBIA, editors, Computational Mechanics Publications, Southampton, Springer-Verlag, Berlin, pp. 355–381.

FALCONER R. A., E. WOLANSKI and L. MARDAPITTA-HADJIPANDELI (1986) Modeling tidal circulation in an island's wake. *Journal of Waterway, Port, Coastal and Ocean Engineering*, **112**, 234–254.

FISCHER H. B., E. Y. LIST, R. C. Y. KOH, J. IMBERGER and N. H. BROOKS (1979) *Mixing in inland and coastal waters*, Academic Press, New York, 484 pp.

GEYER W. R. and R. SIGNELL (1990) Measurements of tidal flow around a headland with a shipboard acoustic Doppler current profiler. *Journal of Geophysical Research*, **95**, 3189–3197.

GREENSPAN H. P. (1968) *The theory of rotating fluids*, Cambridge University Press, New York, 327 pp.

HAMNER W. H. and I. HAURI (1977) Fine-scale currents in the Whitsunday Islands, Queensland, Australia: effect of tide and topography. *Australian Journal of Marine and Freshwater Research*, **28**, 333–359.

HAMNER W. H. and I. HAURI (1981) Effects of island mass: water flow and plankton pattern around a reef in the Great Barrier Reef lagoon, Australia. *Limnology and Oceanography*, **26**, 1084–1102.

HAMNER W. H. and E. WOLANSKI (1988) Hydrodynamic forcing functions and biological processes on coral reefs: a status review. In: *Proceedings 6th international coral reef symposium*, Townsville, 8–12 August, pp. 103–113.

INGRAM R. G. and V. H. CHU (1987) Flow around islands in Rupert Bay: an investigation of the bottom friction effect. *Journal of Geophysical Research*, **92**, 14521–14533.

JAMES I. D. (1986) A front-resolving sigma coordinate sea model with a simple hybrid advection scheme. *Applied Mathematical Modelling*, **10**, 87–92.

LAFOND E. C. and K. G. LAFOND (1971) Oceanography and its relation to marine organic production. In: *Fertility of the sea* (Vol. 1), J. D. COSTLOW JR, editor, Gordon and Breach, New York, pp. 241–254.

MELLOR G. L. and A. F. BLUMBERG (1985) Modeling vertical and horizontal diffusivities with the sigma coordinate system. *Monthly Weather Review*, **113**, 1379–1383.

MESINGER, F. and A. ARAKAWA (1976) *Numerical methods used in atmospheric models*, Vol. 1, GARP Publications Series No. 17, WMO-ICSU Joint Organizing Committee, 64 pp.

NIHOUL J. C. J. (1984) A three-dimensional general marine circulation model in a remote sensing perspective. *Annales Geophysicae*, **4**, 433–442.

NIHOUL J. C. J. and S. DJENIDI (1987) Perspective in three-dimensional modelling of the marine system. In: *Three-dimensional models of marine and estuarine dynamics*, J. C. J. NIHOUL and B. M. JAMART, editors, Elsevier, Amsterdam, pp. 1–33.

NIHOUL J. C. J., E. DELEERSNIJDER and S. DJENIDI (1989) Modelling the general circulation of shelf seas by 3D $k$-$\varepsilon$ models. *Earth-science Reviews*, **26**, 163–189.

PATTIARATCHI C., A. JAMES and M. COLLINS (1987) Island wakes and headland eddies: a comparison between remotely sensed data and laboratory experiments. *Journal of Geophysical Research*, **92**, 783–794.

PINGREE R. D. (1978) The formation of the Shambles and other banks by tidal stirring of the seas. *Journal of the Marine Biological Association of the United Kingdom*, **58**, 211–226.

PINGREE R. D. and L. MADDOCK (1980) The effects of bottom friction and Earth's rotation on an island's wake. *Journal of the Marine Biological Association of the United Kingdom*, **60**, 499–508.

PEYRET R. and T. D. TAYLOR (1983) *Computational methods for fluid flow*, Springer-Verlag, New York, 358 pp.

POWELL T. M. (1989) Physical and biological scales of variability in lakes, estuaries and coastal ocean. In: *Perspectives in ecological theory*, J. ROUGHGARDEN, R. M. MAY and S. A. LEVIN, editors, Princeton University Press, pp. 157–176.

SIGNELL R. P. (1989) Tidals dynamics and dispersion around coastal headlands. Ph.D. Thesis, Woods Hole Oceanographic Institution (WHOI-89-38) and Massachusetts Institute of Technology, 162 pp.

SIGNELL R. P. and W. R. GEYER (1991) Transient eddy formation around headlands. *Journal of Geophysical Research*, **96**, 2561–2575.

TOMCZAK M. (1988) Island wakes in deep and shallow waters. *Journal of Geophysical Research*, **93**, 5153–5154.

VAN SENDEN D. C. (1987) Dynamics of unsteady jets in shallow receiving waters. Ph.D. Thesis, Department of Civil Engineering, The University of Western Australia, 224 pp.

VON RIEGELS F. (1938) Zur Kritik des Hele-Shaw Versuchs. *Zeitschrift für Angewandte Mathematik und Mechanik*, **18**, 95–106.

WOLANSKI E. (1988) Island wakes in shallow waters. *Journal of Geophysical Research*, **93**, 1335–1336.

WOLANSKI E. (1991) Hydrodynamics of tropical coastal marine systems. In: *Pollution in tropical aquatic systems*, D. W. CONNELL and D. W. HAWKER, editors, CRC Press, FL, U.S.A., pp. 3–27.

WOLANSKI E. and W. M. HAMNER (1988) Topographically controlled fronts in the ocean and their biological influence. *Science*, **241**, 177–181.

WOLANSKI E., J. IMBERGER and M. L. HERON (1984) Island wakes in shallow coastal waters. *Journal of Geophysical Research*, **89**, 10553–10569.